JOURNAL OF MATERIALS SCIENCE 29 (1994) 1004–1010

# Non-destructive evaluation of the micromechanism of the deformation process during tensile tests on polymers by the elastic-wave transfer function method

H. KAWABE, Y. NATSUME
*Nippondenso Co. Ltd, 1-1 Showa-cho, Kariya 448, Japan*
Y. HIGO, S. NUNOMURA
*Precision and Intelligence Laboratory, Tokyo Institute of Technology, 4259 Nagatsuta, Midori-ku, Yokohama 227, Japan*

The elastic-wave transfer function method (ETFuM) was applied to make clear the micromechanism of the deformation process during dynamic tensile testing of polymethylmethacrylate (PMMA) and polycarbonate (PC). In PC, the transfer function began to change at a high frequency. After that, it decreased abruptly in the low-frequency region. The variation of the transfer function at high frequency was caused by the nucleation and growth of microdefects such as crazes and microcracks. The variation at low frequency was caused by plastic deformation such as inclined necking and microdefects due to shear stress. On the other hand, in PMMA the transfer function changed homogeneously with elongation at high frequencies and did not change at low frequencies. The variation of the transfer function during tensile testing related to the micromechanism of elastic and plastic deformation processes in both PC and PMMA. The results suggested that the ETFuM is a useful and powerful method for evaluating the micromechanism of deformation processes in polymers in a non-destructive and dynamic way.

## 1. Introduction

Thermoplastic polymers are being used more and more often for applications where considerable loading is involved. Among the factors affecting the static and dynamic properties of materials, the initiation and growth of crazes and microcracks are considered to constitute a precursor stage which begins to affect fundamental properties of materials such as tensile strength, elastic modulus and fracture toughness [1]. These factors affecting the degradation process are considered as the nucleation of irregular structure from the point of view of materials science.

When we consider the fracture process of a polymer, crazes are thought to be a source of microcracking and fracture. Crazes are easy to detect optically. However, the micromechanism of the deformation process of the precursor stage of fracture has not been understood, because of the difficulty of detection and observation. It is an important problem to evaluate these factors quantitatively as a durability evaluation technique in polymers. However, it is difficult to evaluate the phenomenon exactly in the no-load condition because the variation of polymer state is faster than that of metals in the temperature range used. There is therefore a need for real-time and non-destructive measurement as the load is developed, in order to make clear the micromechanism of the deformation process.

Most investigations concerning the micromechanism of the deformation process are conducted under zero load, and it is hard to find research concerning a dynamic evaluation of the micromechanism of the deformation process under loaded conditions. As for the micromechanism of the deformation process which ends in fracture, it is considered that an elastic heterogeneous area will be nucleated in which there are changes of density, acoustic impedance and elastic modulus. Therefore, if this elastic heterogeneous area can be evaluated dynamically and quantitatively in real time, we can carry out dynamic microanalysis during tensile straining of the polymer.

We have been investigating a new non-destructive evaluation method, the elastic-wave transfer function method (ETFuM), in order to make clear the micromechanism of the deformation process in polymer in a quantitative manner [2, 3]. A change of the transfer function is caused by the existence of crazes and microcracks in the material [4–6]. Information about amplitude and phase is gained by analysing the transfer function. Manson [7] measured the attenuation and scattering of a high-frequency sound wave of 2–15 MHz in metals and glasses, and reported that a fourth-power scattering law held quite well until the grain size was equal to one-third of a wavelength; at higher frequencies the scattering loss increased more nearly with the square of the frequency. In addition,


0022–2461 

Kikuchi [8, 9] investigated the propagation of elastic waves in a medium containing many inclusions, and reported that a general equation could be derived for determination of the velocity dispersion and attenuation coefficient of the effective wave under the assumption that the spatial distribution of inclusions was uniform.

In this study, ETFuM is applied to make clear the micromechanism of the deformation process during dynamic tensile testing of polymethylmethacrylate (PMMA) and polycarbonate (PC). This method has the advantage of monitoring the specimen non-destructively and furthermore of evaluating it under operating conditions without removing structural components.

## 2. Experimental procedure

### 2.1. Materials

Commercially available PMMA and PC were used in this study. Both materials are thermoplastic and amorphous polymers. Mechanical properties of the materials need in this study used are given in Table I. Fig. 1 shows the shapes and dimensions of the specimens used. Tensile specimens were machined from extruded sheets of PC and PMMA which had 25 and 20 mm thickness, respectively. All specimens were machined parallel to the rolling direction of the material. The residual stress of the machined specimens was removed by annealing them for 2 h at 80 °C for PMMA and 125 °C for PC, and then cooling in the furnace. To investigate variation of the transfer function with specimen shape, two kinds of specimen were used. A pair of rectangular windows were machined to attach an AE transducer to each side shown as surface A in Fig. 1.

### 2.2. Explanation of ETFuM

From the principles of the transfer system of an elastic wave, the respective functions in the time domain are defined as follow [5]:

$$g(t) = \int_{-\infty}^{+\infty} h(t-\tau)f(t)\,d\tau = h(t) \times f(t) \quad (1)$$

They are then transformed to the frequency domain by performing a Fourier transform operation on the integral equation:

$$G(\omega) = H(\omega) \cdot F(\omega) \quad (2)$$

where $G(\omega)$, $H(\omega)$ and $F(\omega)$ are the respective Fourier transforms of $g(t)$, $h(t)$ and $f(t)$. The input signal path is expected to be as in Fig. 2 and is defined as follows:

$$G_A(\omega) = M \cdot \beta_2 \cdot h_A \cdot S \cdot F(\omega) \quad (3)$$

TABLE I Mechanical properties of polymers tested

| | PMMA | PC |
|---|---|---|
| Relative specific gravity | 1.19 | 1.20 |
| Tensile strength (MPa) | 72.0 | 60.0 |
| Modulus of elasticity (GPa) | 3.4 | 2.3 |
| Deflection temperature (°C) | 89 | 145 |

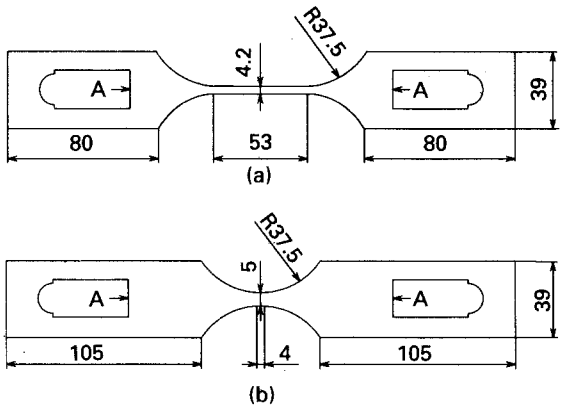


*Figure 1* Shapes and dimensions of test specimen.

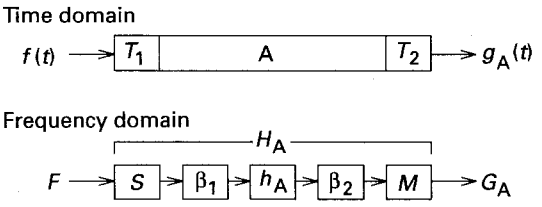


*Figure 2* Schematic diagram showing elastic wave transmission system. $\beta_1$ and $\beta_2$ are coupling factors.

where $M$ and $S$ are respectively the receiver and transmitter transducer sensitivity, and $\beta_1$ and $\beta_2$ the transfer functions of the coupling between transducer and specimen. The transfer function of the elastic signal through the specimen is expressed as

$$H_A(\omega) = G_A(\omega)/F(\omega) = S \cdot \beta_1 \cdot h_A \cdot \beta_2 \cdot M \quad (4)$$

The transfer function $H_A$ is found by multiplying the transfer functions of the system components in the frequency domain as indicated in this equation. We only want to obtain information on the polymer specimen $h_A$, so we need to separate that information from the characteristics of the transducers and the coupling conditions between the transducers and the specimen expressed as $\beta_1$ and $\beta_2$. We will denote the transducers referred to here as S and M. In addition, we have developed a method of coupling the transducer to the specimen so as to obtain good acoustic reproducibility. The transfer function $H_{AN}$ for a different specimen is defined in the same way as $H_{A0}$ for a standard specimen. In this experiment, we denote the transfer function for a virgin specimen as $H_{A0}$. Then all components of the transfer function that reflect the characteristics of the transducers S and M and the coupling conditions $\beta_1$ and $\beta_2$ are cancelled out, leaving only the information on the specimen as follows:

$$\frac{H_{AN}}{H_{A0}} = \frac{G_{AN}/F_N}{G_{A0}/F_0} = \left(\frac{S_N}{S_0}\right)\cdot\left(\frac{\beta_{1N}}{\beta_{10}}\right)\cdot\left(\frac{h_{AN}}{h_{A0}}\right)\cdot\left(\frac{\beta_{2N}}{\beta_{20}}\right)\cdot\left(\frac{M_N}{M_0}\right) = \frac{h_{AN}}{h_{A0}} \quad (5)$$

The signal source F provides good reproducibility. The ratio of the output signal $G_{AN}$ to $G_{A0}$ relates

directly to the corresponding difference in the dynamic property of the specimen:

$$G(\omega) = \frac{G_{AN}}{G_{A0}} = \frac{h_{AN}}{h_{A0}} \quad (6)$$

The effects of specimen shape, transducer sensitivity and so were thus eliminated in Equation 6. The evaluation function $\Delta h_{Af12}$ was then defined as

$$\Delta h_{Af12} = \int_{f_2}^{f_1} |G(\omega)| \, d\omega \quad (7)$$

Here $\Delta h_{Af12}$ is the value integrated over a frequency range from $f_1$ to $f_2$.

## 2.3. Method of measurement

The block diagram of the ETFuM measurement system during a tensile test is shown in Fig. 3. Two piezoelectric transducers were used as transmitter and receiver, respectively. They were put in direct contact with the specimen with couplant grease. The signal F is generated by a function generator and input to the transmitting transducer, passes through the polymer specimen and is picked up by the receiving transducer and amplifier. It is then fed into an FFT analyser along with the input signal at regular intervals during the tensile test until fracture. The signals are compared and only information on the specimen is extracted using Equation 5 or 6. The entire system is controlled automatically by a microcomputer.

Flat-type PZT transducers were employed and the contact agent between the transducers and the specimen was W-400 (Nippon Steel Co.). It provides good reproducibility of the mounting condition, for both the amplitude and phase components [10]. The measured data obtained with these transducers were sufficiently reliable for comparison without performing any special sensitivity calibration.

The tensile tests were performed at 0.1 mm min$^{-1}$ crosshead speed on an Instron-type testing machine. The tensile specimen was supported by loading pins. During a tensile test the displacement between each transducer was measured by a linear variable differential transformer (LVDT). After a test the transfer function was calculated from the input and output signals recorded in the FFT analyser, and compared with load and elongation. The surface behaviour was observed under tensile stress by an optical microscope. The longitudinal wave velocity was also measured, using a 1 MHz pulse wave and an acoustic emission measuring system. All tests were performed at room temperature.

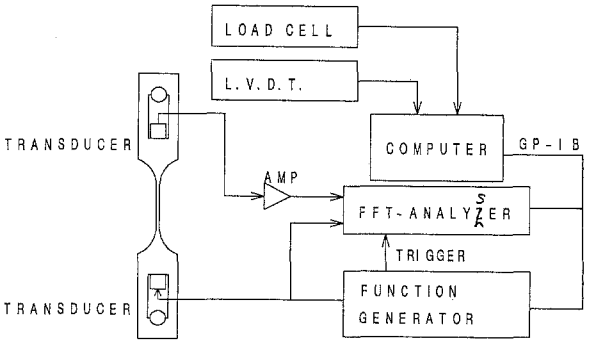


*Figure 3* Block diagram of ETFuM measuring system.

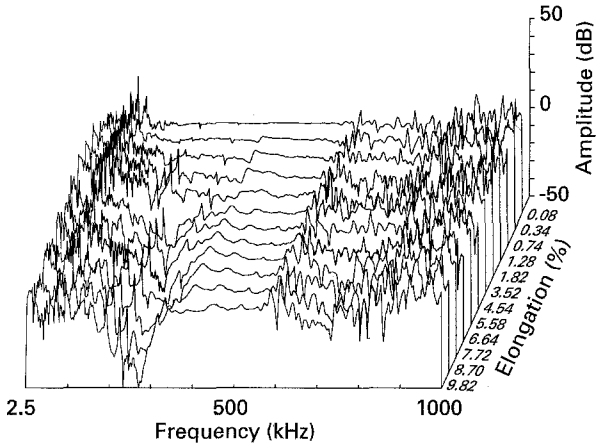


*Figure 4* Variation of transfer function with frequency during tensile testing of PC, shown at different elongations. Data over 600 kHz are noise. In this figure the amplitude varied in the region 100–600 kHz.

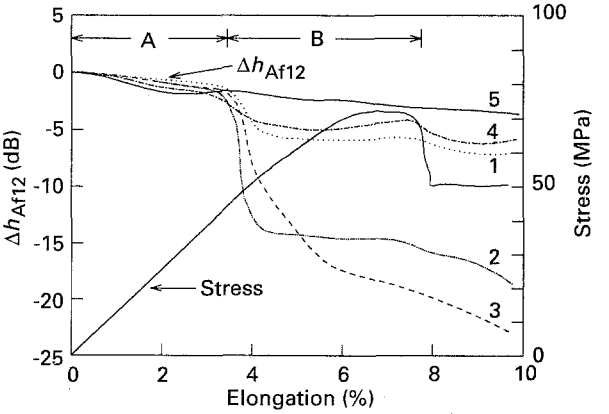


*Figure 5* Relation between $\Delta h_{Af12}$, tensile stress and elongation during tensile testing of PC: (1) 150–200 kHz, (2) 200–250 kHz, (3) 250–300 kHz, (4) 500–550 kHz, (5) 550–600 kHz. At first (domain A), $\Delta h_{Af12}$ began to change in the high-frequency range 500–600 kHz. After that (domain B), $\Delta h_{Af12}$ decreased abruptly in the low-frequency range 200–300 kHz.

## 3. Results

Fig. 4 shows the variation of the transfer function with frequency during a tensile test of PC. The results are shown for various values of elongation. Data over 600 kHz are noise because the signal was too attenuated. In this figure the amplitude varied in the range 100–600 kHz. The results in Fig. 4 were obtained from a specimen shaped as in Fig. 1a, but the results obtained from a different specimen were similar.

In order to evaluate the transfer function quantitatively, the difference of attenuation $\Delta h_{Af12}$ was analysed using Equation 7. Fig. 5 shows the relation between $\Delta h_{Af12}$, tensile stress and elongation. After elastic deformation the specimen yielded, then necking initiated and finally the specimen failed. Meanwhile $\Delta h_{Af12}$ decreased with increasing elongation. At first (domain A), $\Delta h_{Af12}$ began to change in the high frequency range of 500–600 kHz. After that, in domain

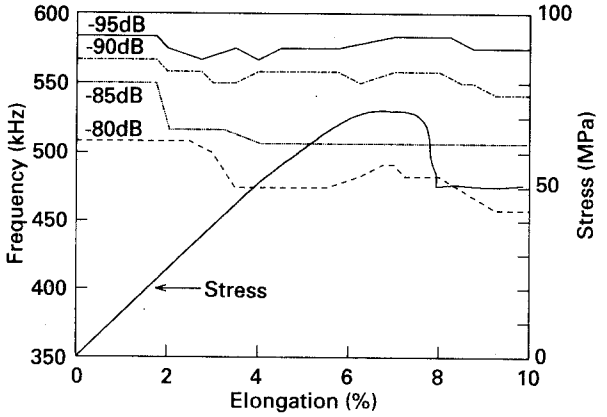


*Figure 6* Frequency change of equivalent amplitude lines of the transfer function during tensile testing of PC. The equivalent amplitude lines of $-80$ and $-85$ dB shifted to low frequency with increasing elongation.

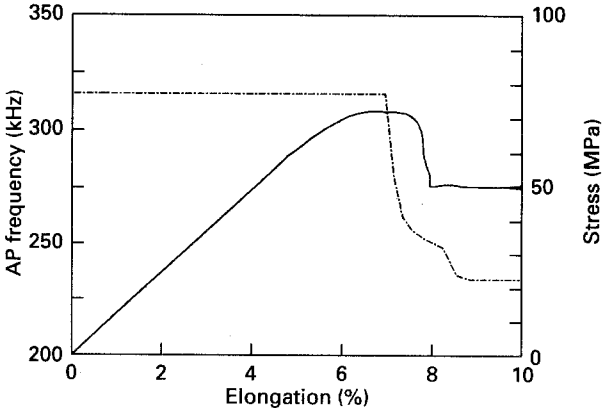


*Figure 7* The relation between elongation and AP frequency at 150–320 kHz during tensile testing of PC: (–·–) AP frequency, (——) stress. The AP frequency was constant at 315 kHz until maximum tensile stress, but began to shift abruptly to lower frequency just after maximum tensile stress, and it was constant again at 232 kHz after the stress was constant.

B $\Delta h_{Af12}$ decreased abruptly in the low-frequency range of 200–300 kHz. In other words, attenuation of the elastic wave strongly increased in this frequency range. In this stage, local orientation of molecular chains has been observed by scanning acoustic microscopy and X-ray diffraction [4]. This suggests that the decrease of the transfer function, in other words attenuation of the elastic wave, was caused by local orientation in very small areas such as the nucleation points of crazes. The reason for variation of the attenuation after yielding is considered to be the nucleation, growth and coalescent of crazes. Furthermore, a plastic deformation area like a Luders band was generated and microcracks were observed in this area, and finally they grew to nearly 1 mm length just before fracture. We call this deformation "inclined necking."

We first analyse the variation of the transfer function in domain A. Fig. 6 shows the relation between elongation and changes of the equivalent amplitude lines in the different frequency domains from Equation 4, in order to analyse the variation of the transfer function in the range 350–600 kHz. The vertical axis indicates the frequency change of equivalent amplitude lines during the tensile test; the stress is also shown. The equivalent amplitude lines of $-80$ and $-85$ dB shifted to low frequency with increasing elongation. This trend corresponds to the variation over 350–600 kHz in Fig. 5. The equivalent amplitude lines began to shift earlier than the start of plastic deformation.

Next, in order to make clear the variation of the transfer function in domain B, the frequency of the attenuation peak (AP) was analysed in the range 150–320 kHz. Fig. 7 shows the relation between elongation and AP frequency. Though the AP frequency was constant at 315 kHz until maximum tensile stress, it began to shift abruptly to a lower frequency just after maximum tensile stress, and it was constant again at 232 kHz after the stress was constant.

In order to make clear the relation between the transfer function and reversible/irreversible properties of the micromechanism of the deformation process in

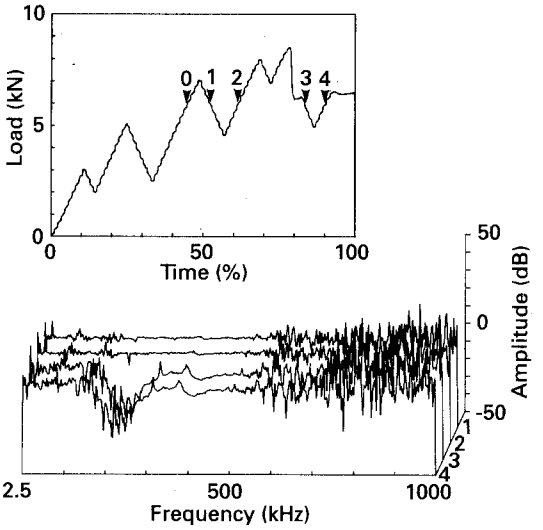


*Figure 8* Comparison of transfer functions under the same load for PC. The vertical axis indicates the variation of the transfer function from Nos 1 to 4 under the same load, normalized to the transfer function of No. 0. The numbers correspond to numbers of loading hystereses.

domains A and B, the transfer function measured before and after inclined necking under the same load is shown in Fig. 8. Loading hysteresis is also shown. The vertical axis indicates the variation of the transfer function from No. 1 to No. 4 under the same load, normalized the transfer function of No. 0, where the numbers correspond to number of loading hystereses. In Nos 1 and 2, irreversible properties were generated since the transfer function changed in a wide frequency range of 50–600 kHz. Comparing before and after inclined necking in Nos 3 and 4, the change at low frequency was clear. Plastic deformation like inclined necking was therefore indicated as an irreversible property.

In PC, inclined necking initiated at maximum tensile stress was observed by optical microscopy. At first, inclined necking began to grow on the specimen (Fig. 9a). After inclined necking extended over the whole specimen, a crack initiated in the direction

perpendicular to the applied stress in the inclined necking area, and it propagated and ended up as a fracture (Fig. 9b).

## 4. Discussion

We discuss the variation of the transfer function in the frequency domain in terms of the propagating properties of an elastic wave in a solid. It is considered that the energy of the elastic wave is attenuated by diffusion loss, scattering at boundaries internal friction and so on [11]. It is considered that the transfer function is influenced by texture variation due to the nucleation of microdefects during tensile testing, since the transfer function evaluated only change from the initial state from Equation 6 in this study. As one mode of texture change, the scattering at a boundary is considered. Under the assumption that the polymer is a polycrystal, the attenuation coefficient $\gamma$ is as follows:

$$\lambda/d > 1: \gamma = ad^3 f^4 \quad (8a)$$

$$\lambda/d \simeq 1: \gamma = bdf^2 \quad (8b)$$

$$\lambda/d < 1; \gamma = c/d \quad (8c)$$

where $d$ is the average grain diameter, $f$ the frequency and $a$, $b$, $c$ are constants.

After elastic deformation the specimen yielded, then necking initiated and finally the specimen failed. Meanwhile $\Delta h_{Af12}$ decreased with increasing elongation. At first, $\Delta h_{Af12}$ began to change in the high-frequency range 500–600 kHz. After that, $\Delta h_{Af12}$ decreased abruptly in the low-frequency range 200–300 kHz. The tensile process is divided into the two regions of elastic deformation (domain A) and plastic deformation (domain B) in Fig. 5.

We first discuss the variation of the transfer function in domain A. We reported that the micromechanism of the deformation process before crazing was as follows [4]. Molecular chains were locally oriented in a very small area with increasing stress. The texture therefore became heterogeneous and anisotropic. It is considered that fibrillar structure is constructed in locally oriented areas which are thought to be embryonic crazing. Since the transfer function changed at a high frequency in Fig. 6, it is suggested that locally oriented areas increased and the elastic wave was scattered at the boundaries between oriented and unoriented areas.

Since the transfer function was attenuated at 500–600 kHz, the corresponding wavelength is 3.6–4.3 mm from the longitudinal wave velocity (2160 m $s^{-1}$). This size is bigger than the size of the supposed defects. For this reason it is considered that the attenuation corresponds not to the size of each defect but to the size of the high-density defect zone. The variation of the transfer function at 500–600 KHz therefore depended on the nucleation and growth of microdefects from (Equation 8a).

Next we discuss domain B. Though crazes at inclined necking areas were observed [5], the transfer function began to change before crazing. Some crazes were therefore nucleated before being observed by optical microscopy. The attenuation of the transfer function after inclined necking is thought to be due to the growth and coalescence of macrocracks. Macrocracks grew nearly 1 mm in length in the direction perpendicular to the applied stress before fracture. In the low-frequency zone 150–320 kHz, the AP frequency began to shift abruptly at maximum tensile stress. At this moment, inclined necking began to initiate and the AP frequency continued to shift until the end of inclined necking growth. According to the relation between wavelength and size of necking, the size of inclined necking was 1–2 mm at the beginning and 25 mm at the end. The wavelength was 6.7–13.5 mm at 160–320 kHz, which corresponds to the size of necking from Equation 8b.

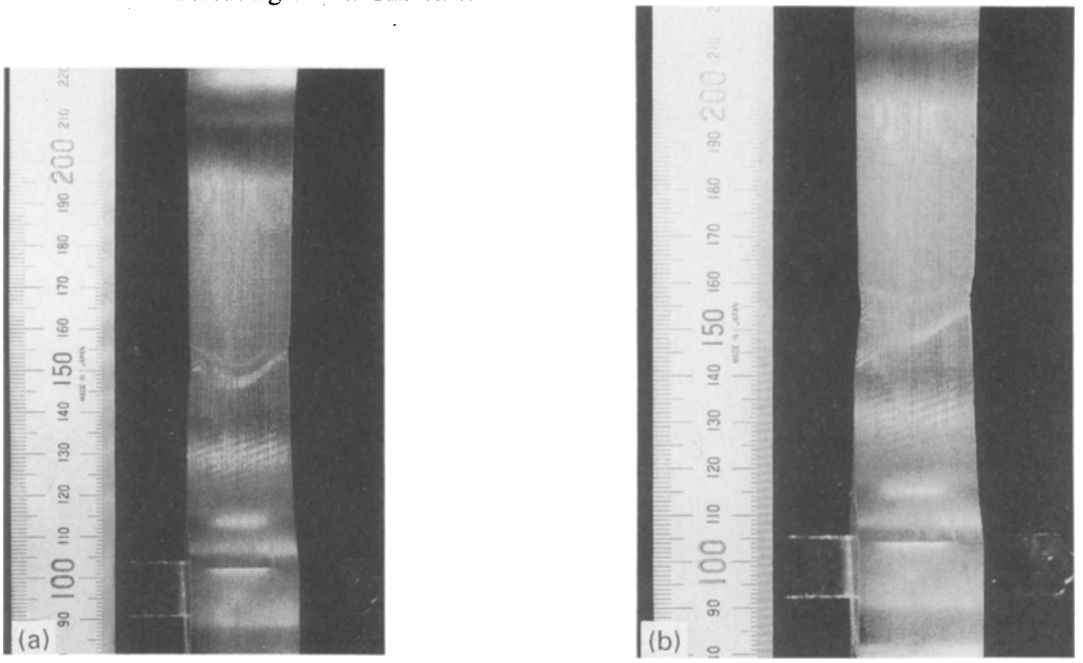


*Figure 9* Optical micrograph of inclined necking in PC. (a) Inclined necking beginning to grow on the specimen. (b) After necking extended over the whole specimen, a crack initiated in the direction perpendicular to the applied stress in an inclined necking area.

The direction of inclined necking growth is given by solution of Equations 9 and 10 below. Equations 9 are equilibrium equations under plain stress, and Equation 10 is the von Mises yield condition:

$$\frac{\partial \sigma_x}{\partial_x} + \frac{\partial \tau_{xy}}{\partial_y} = 0 \qquad (9)$$

$$\frac{\partial \tau_{xy}}{\partial_x} + \frac{\partial \sigma_y}{\partial_y} = 0$$

$$\sigma_x^2 - \sigma_x \sigma_y + \sigma_y^2 + 3\tau_{xy} = 3k^2 \qquad (10)$$

where $\sigma_x$, $\sigma_y$ and $\sigma_z$ are the principal stresses and $k$ is constant due to the materials. Under plain stress, $\sigma_z = \tau_{yz} = \tau_{zx} = 0$. From Equations 9 and 10

$$\theta = \tan^{-1} \left\{ 3\tau_{xy} \pm \frac{[(\sigma_x - 2\sigma_y)(2\sigma_x - \sigma_y) + 9\tau_{xy}]^{1/2}}{\sigma_x - 2\sigma_y} \right\}$$

Under uniaxial stress, $\sigma_y = \tau_{xy} = 0$ and

$$\theta = \tan^{-1}(\pm 2^{1/2}) = 54.7^\circ$$

This angle agreed quite well with the experimental values. It was therefore considered that inclined necking was caused by maximum shear stress.

Next, we discuss the relation between the transfer function and reversible/irreversible properties of the micromechanism of deformation process in domains A and B. Since the transfer function of Nos 1 and 2 in Fig. 8 changed in a wide frequency range, it indicated irreversible properties. It was caused by the nucleation of microdefects which had remained after unloading. The variation of the transfer function of No. 2 was a little bigger than that of No. 1. The reason for this is thought to be an increase of irreversible properties accompanying cyclic loading. Comparing before and after inclined necking in Nos 3 and 4, a variation at low frequency is clearly indicated. Therefore plastic deformation like necking was indicated as an irreversible property.

In order to compare the variation of the transfer function in different materials which end with brittle fracture, the variation of the transfer function in PMMA is shown in Fig. 10. The stress increased linearly with elongation and the specimen failed without inclined necking in PMMA. $\Delta h_{Af12}$ changed homogeneously with elongation at high frequencies of 0.5–1.2 MHz. These results correspond with the results in domain A of Fig. 5. Since the attenuation was stronger in the higher frequency range, the higher frequency range is more sensitive to fine craze nuclei. In order to compare the relation between the transfer function and reversible/irreversible properties in PMMA, the transfer function measured before and after inclined necking under the same load is shown in Fig. 11. Loading hysteresis is also shown. The vertical axis indicates the variation of the transfer function from No. 1 to No. 4 under the same load, normalized to the transfer function of No. 0. The numbers correspond to numbers of loading hystereses. Though small irreversible properties were generated in a wide frequency range, a change at low frequency was not observed. These were different from the results for PC. However, the variation of the transfer function increased a little with cyclic loading as in Fig. 8, and this was thought to show an increase of irreversible properties, in other words an accumulation of microdefects.

The micromechanism of the deformation process of a polymer is schematically drawn in Fig. 12. Fig. 12a–c are schematic figures showing the nucleation and growth of inclined necking like a Luders band during tensile testing. Fig. 12d shows microdefects like crazes and microcracks caused by shear stress. The variation of the transfer function at high frequency is caused by the nucleation and growth of microdefects like crazes and microcracks. The variation in low frequency is caused by plastic deformation like inclined necking and microdefects due to shear stress, which could not be observed in this study. Since the transfer function did not change at low frequency in PMMA, it is considered that only the

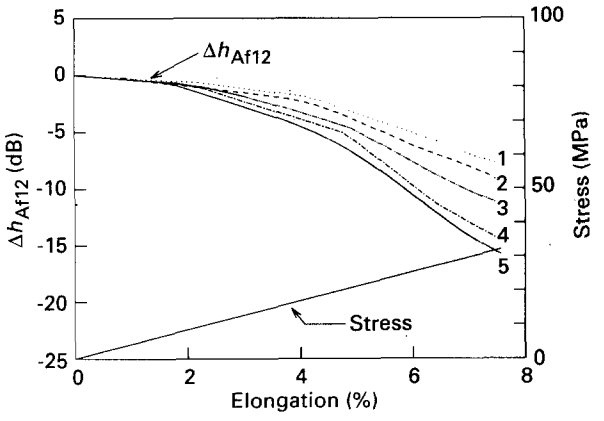


*Figure 10* Variation of the transfer function during tensile testing of PMMA: (1) 200–400 kHz, (2) 400–600 kHz, (3) 600–800 kHz, (4) 800–1000 kHz, (5) 1000–1200 kHz. Stress increased linearly with elongation and the specimen failed without necking. $\Delta h_{Af12}$ changed homogeneously with elongation from high frequencies of 0.5–1.2 MHz.

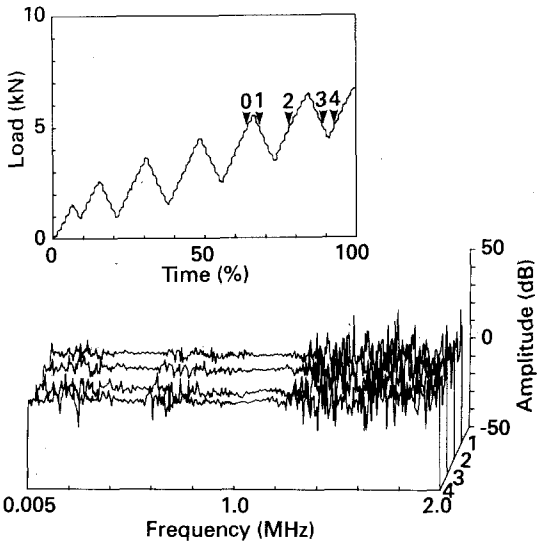


*Figure 11* Comparison of the transfer function under the same load in PMMA. The vertical axis indicates the variation of the transfer function from No. 1 to No. 4 under the same load, normalized to the transfer function of No. 0. The numbers correspond to numbers of loading hystereses. No change at low frequency was measured, in contrast to the results for PC.

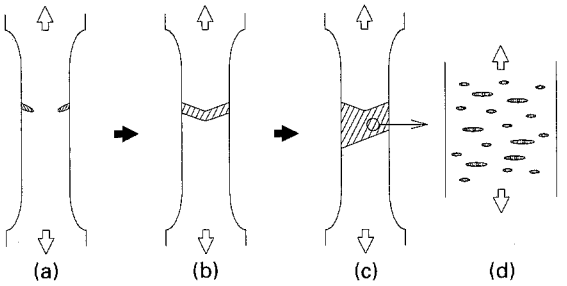


*Figure 12* (a–c) Schematic figures of nucleation and growth of inclined necking during tensile testing; (d) microdefects like crazes and microcracks caused by shear stress.

nucleation and growth of microdefects were generated. All the results suggested that the variation of the transfer function during tensile testing corresponded to the micromechanism of elastic and plastic deformation processes in both PC and PMMA.

## 5. Conclusions

ETFuM was applied to make clear the micromechanism of the deformation process during dynamic tensile testing in PMMA and PC.

1. In PC, the transfer function began to change in the high-frequency range 500–600 kHz. After that it decreased abruptly in the low-frequency range 200–300 kHz. The variation of the transfer function at high frequency is caused by the nucleation and growth of microdefects like crazes and microcracks. The variation at low frequency is caused by plastic deformation like inclined necking and by microdefects due to shear stress.

2. The transfer function was measured in PMMA which ended up in a brittle fracture. The transfer function changed homogeneously with elongation at high frequencies of 0.5–1.2 MHz, and did not change at low frequency. It is therefore considered that only the nucleation and growth of microdefects were generated in PMMA.

3. The variation of the transfer function during tensile testing was related to the micromechanism of elastic and plastic deformation processes in both PC and PMMA. The results suggested that the ETFuM is a useful and powerful method for evaluating the micromechanism of the deformation process of a polymer, both non-destructively and dynamically.

## References

1. I. NARISAWA, "Materials Strength in Plastics" (in Japanese) (Ohm Press, Tokyo, 1982) 163.
2. Y. HIGO and S. NUNOMURA, in Proceedings of 2nd Symposium on Non-destructive Evaluation in New Materials and Products, Tokyo (1988) 131.
3. Y. HUSHIMI and A. WADA, *Rev. Sci. Instrum.* **47**(2) (1976) 213.
4. H. KAWABE and Y. HIGO, *J. Mater. Sci.* **27** (1992) 5547.
5. *Idem*, in "Nondestructive Characterization of Material V, Tokyo (1992) 745.
6. *Idem., J. Mater. Sci.* in press.
7. W. P. MANSON, *J. Acoust. Soc. Amer.* **19** (1947) 464.
8. M. KIKUCHI, *Phys. Earth & Plan. Inter.* **25** (1981) 159.
9. *Idem, ibid.* **27** (1981) 100.
10. Y. HIGO and M. ONO, in "Progress in A.E.", Vol. 3 (Japan Society of Non-Destructive Inspection, Tokyo, 1986) p. 685.
11. "Ultrasonic Technology Manual" (in Japanese) (Nikkan Kogyo Shimbun Ltd., Tokyo, 1978).

*Received 11 March*
*and accepted 24 August 1993*